

STEADY FLOW NEAR A WEDGE SHAPED BOW

E. FONTAINE

Ecole Centrale de Nantes, 1 rue de la Noë, 44072 Nantes Cedex, France.

O.M. FALTINSEN

Division of Marine Hydrodynamics,
Norwegian University of Science and Technology, N-7034 Trondheim, Norway.

1 Introduction

The free surface steady potential flow around a fine wedge shaped bow is studied. The concept of a bow flow solution was first introduced by Ogilvie (1972) and has recently been studied by (among others) Faltinsen & Zhao (1991), Fontaine & Cointe (1997), and Fontaine (1996). When the so called $2D + 1/2$ or $2D + t$ theory is used to find the bow solution, good agreement is generally reported between the measured and computed wave profile along the hull. The main differences appear at the "nose" (apex) of the wedge where an initial elevation is observed but is not predicted. To overcome this misfit, a local analysis of the flow in the near-bow domain is performed (see fig. 1). The near-bow solution matches on the one hand to the bow-flow solution and on the other hand to the far-field solution. It also leads to an estimate of the wave elevation at the nose of the bow. Comparison with experiments are given. Extension of the theory to general cross-sections will be discussed in the oral presentation.

2 The near-bow flow

The two non-dimensional parameters describing the wedge shaped bow are $\tan \alpha = b/L$ and $\delta = h/L$. The near-bow domain is based on a length scale equal to the draft h and a velocity scale equal to U . The non-dimensional variables are defined as :

$$\hat{x} = \frac{x}{h}, \quad \hat{y} = \frac{y}{h}, \quad \hat{z} = \frac{z}{h}, \quad \hat{\varphi} = \frac{\varphi}{Ub}, \quad \hat{\eta} = \frac{\eta}{b}$$

where φ is the velocity perturbation potential and η the free surface elevation. Assuming the ship to be slender or thin ($\alpha \ll 1$, $\delta \ll 1$), the following asymptotic expansions are introduced :

$$\hat{\varphi}(\hat{x}, \hat{y}, \hat{z}; \alpha, \delta) = \check{\nu}_1(\alpha, \delta) \check{\varphi}_1(\hat{x}, \hat{y}, \hat{z}) + o(\check{\nu}_1)$$

$$\hat{\eta}(\hat{x}, \hat{y}; \alpha, \delta) = \check{\nu}_1(\alpha, \delta) \check{\eta}_1(\hat{x}, \hat{y}) + o(\check{\nu}_1)$$

Since there is no dilation of the space variables, the leading order perturbation potential $\check{\varphi}_1$ satisfies the three-dimensional Laplace equation in the fluid domain. Using the non-dimensional variables, the body boundary condition gives :

$$(1 + \check{\mu}_1 \frac{\partial \check{\varphi}_1}{\partial \hat{x}}) - \frac{\check{\mu}_1}{\delta} \frac{\partial \check{\varphi}_1}{\partial \hat{y}} + o(1) = 0$$

The principle of least degeneracy implies that $\check{\mu}_1 = \delta$. When the ship is thin ($\alpha \ll \delta$), the resulting condition is :

$$\frac{\partial \check{\varphi}_1}{\partial \hat{y}}(\hat{x}, 0, \hat{z}) = 1 \quad (1)$$

on the center plane of the hull.

The kinematic free surface condition is imposed on $\hat{z} = (\alpha/\delta) \check{\nu}_1 \check{\eta}_1$ and takes the form :

$$(1 + \tan \alpha \frac{\partial \check{\varphi}_1}{\partial \hat{x}}) \frac{\partial \check{\eta}_1}{\partial \hat{x}} + \tan \alpha \frac{\partial \check{\varphi}_1}{\partial \hat{y}} \cdot \frac{\partial \check{\eta}_1}{\partial \hat{y}} - \frac{\delta}{\check{\nu}_1} \frac{\partial \check{\varphi}_1}{\partial \hat{z}} + o(1) = 0$$

The principle of least degeneracy implies that $\check{\nu}_1 = \delta$ so that the resulting condition at first order is :

$$\left[\frac{\partial \check{\eta}_1}{\partial \hat{x}} - \frac{\partial \check{\varphi}_1}{\partial \hat{z}} \right](\hat{x}, \hat{y}, 0) = 0 \quad (2)$$

The dynamic free-surface condition is then :

$$\frac{\partial \check{\varphi}_1}{\partial \hat{x}} + \frac{1}{2} \tan \alpha \left(\left(\frac{\partial \check{\varphi}_1}{\partial \hat{x}} \right)^2 + \left(\frac{\partial \check{\varphi}_1}{\partial \hat{y}} \right)^2 + \left(\frac{\partial \check{\varphi}_1}{\partial \hat{z}} \right)^2 \right) + \tan \alpha \frac{gL}{U^2} \check{\eta}_1 + o(1) = 0 \quad (3)$$

Since $\check{\eta}_1$ is of order $O(1)$, a non-trivial solution can then only be found if :

$$\frac{gL}{U^2} \leq O\left(\frac{1}{\tan \alpha}\right) \quad (4)$$

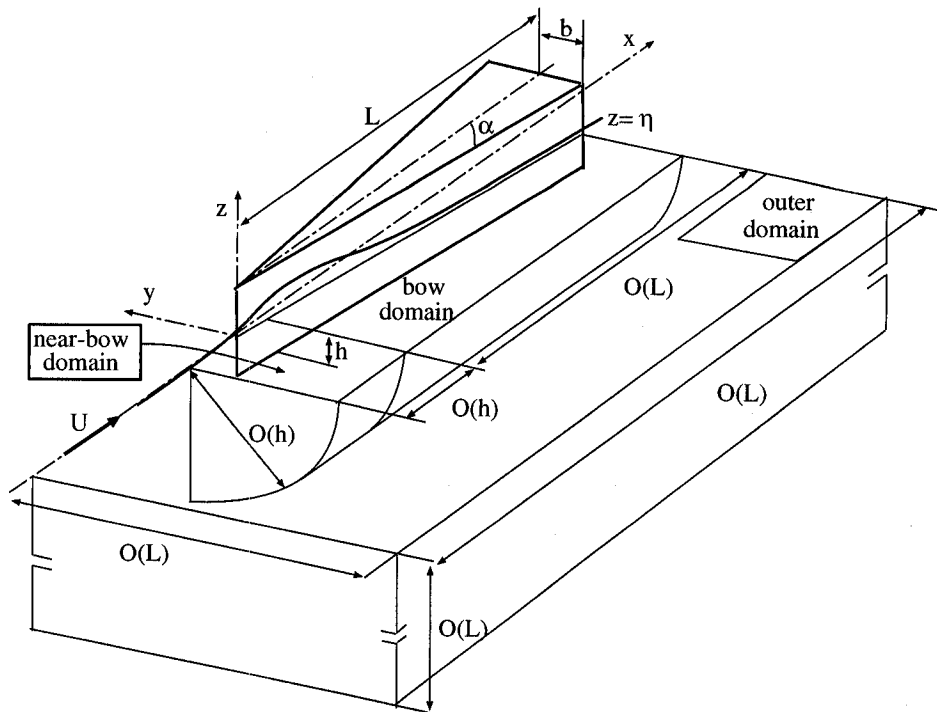


Figure 1: illustration of the different domains of the composite solution.

Fontaine & Cointe (1997) obtained a similar condition for the different approximations to be coherent in the bow flow problem :

$$\frac{gL}{U^2} \leq O(\delta) \quad (5)$$

Since we study both the bow flow and the near-bow flow, we must satisfy the condition (5) which is the more restrictive. In that case, $2D+t$ theory can be used to compute the bow solution and the previous near-bow approximations remain valid. As a consequence, gravity effect can be neglected at first order in equation (3). Assuming the perturbation potential vanishes at infinity in front of the ship ($\hat{x} \rightarrow -\infty$), the resulting condition is :

$$\check{\varphi}_1(\hat{x}, \hat{y}, 0) = 0 \quad (6)$$

The perturbation potential satisfies the three-dimensional Laplace equation subject to the boundary conditions (1) and (6). The solution of this problem can be expressed in term of a distribution on the center plane of the hull of Rankine sources and mirror sinks above $\hat{z} = 0$:

$$\check{\varphi}_1 = \lim_{\delta \rightarrow 0} \frac{1}{2\pi} \int_{-1}^0 d\zeta \int_0^{L/\delta} d\xi G(\hat{x}, \hat{y}, \hat{z}, \xi, 0, \zeta)$$

$$\text{with : } G = [(\hat{x} - \xi)^2 + \hat{y}^2 + (\hat{z} + \zeta)^2]^{-1/2} - [(\hat{x} - \xi)^2 + \hat{y}^2 + (\hat{z} - \zeta)^2]^{-1/2}$$

Taking the limit and performing the integral leads to :

$$\check{\varphi}_1 = \frac{1}{2\pi} \int_{-1}^0 \ln \left[\frac{-\hat{x} + \sqrt{\hat{x}^2 + \hat{y}^2 + (\hat{z} - \zeta)^2}}{-\hat{x} + \sqrt{\hat{x}^2 + \hat{y}^2 + (\hat{z} + \zeta)^2}} \right] d\zeta \quad (7)$$

3 Matching of the different solutions

Fontaine & Cointe (1997) use the method of matched asymptotic expansions to define an inner solution valid in the bow region, and an outer solution valid far from the ship. Even if the outer solution remains valid in front of the ship, these two solutions are not of same order of magnitude in the near-bow domain so that they do not match at first order (Fontaine, 1996). The introduction of the near-bow domain removes this gap since the near-bow solution matches on the one hand to the bow flow solution and on the other hand to the far-field solution.

Using the following non-dimensional variables :

$$\tilde{x} = \frac{x}{L}, \quad \tilde{y} = \frac{y}{L}, \quad \tilde{z} = \frac{z}{L}, \quad \tilde{r} = \sqrt{\tilde{y}^2 + \tilde{z}^2},$$

the perturbation potential is given by¹ :

$$\frac{\varphi}{Ub} = \begin{cases} \delta \tilde{\varphi}_1(\tilde{x}, \tilde{y}, \tilde{z}) & \text{in the near-bow domain} \\ \delta \hat{\varphi}_1(\tilde{x}, \tilde{y}, \tilde{z}) & \text{in the bow domain} \\ \delta^2 \tilde{\varphi}_1(\tilde{x}, \tilde{y}, \tilde{z}) & \text{in the far-field domain} \end{cases}$$

The far-field solution is given by a distribution of three-dimensional vertical dipoles on the axis $\tilde{x} \geq 0$. Using $\theta = \tan^{-1}(\tilde{z}/\tilde{y})$, $\tilde{\varphi}_1$ is given by :

$$\tilde{\varphi}_1(\tilde{x}, \tilde{r}, \theta) = \int_0^\infty \frac{-\mu(s)}{4\pi} \frac{\tilde{r} \sin(\theta)}{[(\tilde{x}-s)^2 + \tilde{r}^2]^{\frac{3}{2}}} ds \quad (8)$$

The dipole density is given by the behaviour of the bow flow solution as $\hat{r} \rightarrow +\infty$:

$$\lim_{\hat{r} \rightarrow \infty} \hat{\varphi}_1(\tilde{x}, \hat{r}, \theta) = -\frac{\mu(\tilde{x})}{2\pi} \cdot \frac{\sin(\theta)}{\hat{r}} \quad (9)$$

3.1 Matching of the near-bow and bow solutions

In order to match the near-bow flow solution to the bow flow one, we define an intermediate variable $x_\chi = \tilde{x}/\chi(\delta)$ where $\delta \ll \chi(\delta) \ll 1$. x_χ is of order $O(1)$ in the overlap domain and the matching condition at first order is :

$$\lim_{\substack{\delta \rightarrow 0 \\ x_\chi > 0 \\ x_\chi = O(1)}} \left[\tilde{\varphi}_1\left(\frac{\chi(\delta)}{\delta} x_\chi, \hat{y}, \hat{z}\right) - \hat{\varphi}_1(\chi(\delta) x_\chi, \hat{y}, \hat{z}) \right] = 0$$

This condition states that the behaviour of the bow solution at origin must be the same as the behaviour of the near-bow solution as $\hat{x} \rightarrow +\infty$. Taking (7) into account, this condition implies that :

$$\hat{\varphi}_1(0, \hat{y}, \hat{z}) = \frac{1}{2\pi} \int_{-1}^0 \ln \left[\frac{\hat{y}^2 + (\hat{z} - \zeta)^2}{\hat{y}^2 + (\hat{z} + \zeta)^2} \right] d\zeta \quad (10)$$

This can be recognised as a solution of the bow flow problem. Indeed, this expression satisfies the two-dimensional Laplace equation subject to the body boundary condition and an homogeneous Dirichlet condition on the unperturbed free-surface. As a result, the two solutions match if the initial conditions for the bow flow problem are :

$$\hat{\varphi}_1(0, \hat{y}, 0) = 0 \quad \text{and} \quad \hat{\eta}_1(0, \hat{y}) = 0$$

These are the same initial conditions as used in the bow flow solution by Fontaine & Cointe (1997) and Faltinsen & Zhao (1991). However, this matching is more precise since the bow flow and the near-bow flow solutions have the same order of magnitude in the overlap domain. As we will see in section 4, it also leads to an initial wave elevation.

¹where the subscript 1 indicates that the quantity is of order $O(1)$

3.2 Matching of the near-bow and far-field solutions

3.2.1 Bow side matching

The behaviour of the near-bow solution far aside the ship bow (as $\hat{x} = O(1)$ and $\hat{r} \rightarrow +\infty$) must be the same as the behaviour of the far-field solution in the vicinity of the ship bow side, i.e. as $\tilde{r} \rightarrow 0$. As before, we define an intermediate variable $r_\chi = \tilde{r}/\chi(\delta)$ ($\delta \ll \chi(\delta) \ll 1$) which is of order $O(1)$ in the overlap domain. The matching condition is at first order :

$$\lim_{\substack{\delta \rightarrow 0 \\ r_\chi = O(1)}} \left[\tilde{\varphi}_1\left(\hat{x}, \frac{\chi(\delta)}{\delta} r_\chi, \theta\right) - \delta \tilde{\varphi}_1(\delta \hat{x}, \chi(\delta) r_\chi, \theta) \right] = 0$$

When $\delta \rightarrow 0$, it follows from (7) and (8) that :

$$\begin{aligned} \tilde{\varphi}_1\left(\hat{x}, \frac{\chi(\delta)}{\delta} r_\chi, \theta\right) &= \frac{1}{2\pi} \frac{\delta}{\chi(\delta)} \frac{\sin \theta}{r_\chi} + O\left[\frac{\delta^2}{\chi(\delta)^2}\right] \\ \delta \tilde{\varphi}_1(\delta \hat{x}, \chi(\delta) r_\chi, \theta) &= -\frac{\mu(0)}{4\pi} \frac{\delta}{\chi(\delta)} \frac{\sin \theta}{r_\chi} + o\left[\frac{\delta}{\chi(\delta)}\right] \end{aligned}$$

The dipole density $\mu(0)$ is determined by using equations (9) and (10). This leads to $\mu(0) = -2$ so that the two solutions match.

3.2.2 Matching in front of the bow

The behaviour of the near-bow flow solution far ahead of the bow, as $\hat{r} = O(1)$ and $\hat{x} \rightarrow -\infty$ must equal the behaviour of the far-field solution in front of the bow (as $\tilde{x} \rightarrow 0^-$). Using an intermediate variable $x_\chi = \tilde{x}/\chi(\delta)$ so that $\delta \ll \chi(\delta) \ll 1$, the matching condition is at first order :

$$\lim_{\substack{\delta \rightarrow 0 \\ x_\chi = O(1) \\ x_\chi < 0}} \left[\tilde{\varphi}_1\left(\frac{\chi(\delta)}{\delta} x_\chi, \hat{r}, \theta\right) - \delta \tilde{\varphi}_1(\chi(\delta) x_\chi, \delta \hat{r}, \theta) \right] = 0$$

When $\delta \rightarrow 0$, it follows from (7) and (8) that :

$$\begin{aligned} \tilde{\varphi}_1\left(\frac{\chi(\delta)}{\delta} x_\chi, \hat{r}, \theta\right) &= \frac{1}{4\pi} \frac{\delta^2}{\chi(\delta)^2} \frac{\hat{r} \sin \theta}{x_\chi^2} + o\left[\frac{\delta^2}{\chi(\delta)^2}\right] \\ \delta \tilde{\varphi}_1(\chi(\delta) x_\chi, \delta \hat{r}, \theta) &= -\frac{\mu(0)}{8\pi} \frac{\delta^2}{\chi(\delta)^2} \frac{\hat{r} \sin \theta}{x_\chi^2} + o\left[\frac{\delta^2}{\chi(\delta)^2}\right] \end{aligned}$$

As a result, the two solutions match.

4 Composite solution

The composite solution is obtained by adding the near-bow to the bow solution and by subtracting the common part (given by eq. (10) for the potential). In front of the bow ($\hat{x} < 0$), the composite solution for the wave elevation is equal to the near-bow solution and can be found by integrating the kinematic free-surface condition (2) :

$$\tilde{\eta}_1(\hat{x} < 0, \hat{y}) = \frac{1}{\pi} \left[\hat{x} \ln \left(\frac{\hat{x} + \sqrt{\hat{x}^2 + \hat{y}^2}}{\hat{x} + \sqrt{\hat{x}^2 + \hat{y}^2 + 1}} \right) + \sqrt{\hat{x}^2 + \hat{y}^2} - \sqrt{\hat{x}^2 + \hat{y}^2 + 1} \right]$$

The wave elevation in front of the bow is therefore independent of the speed and the wave elevation at the nose is :

$$\eta(0, 0) = \frac{\alpha h}{\pi} \quad (11)$$

These results differ from the results of Sclavounos (1994). He predicted half the value of eq. (11). The theoretical result has been compared with experiments presented by Fontaine (1996). Because of the small size of the tested model, the effect of surface tension is important. The experimental results can be scaled to full scale by introducing a surface tension parameter (see fig. 2). Full scale corresponds to that surface tension parameter goes to zero. The results show that eq. (11) is reasonable.

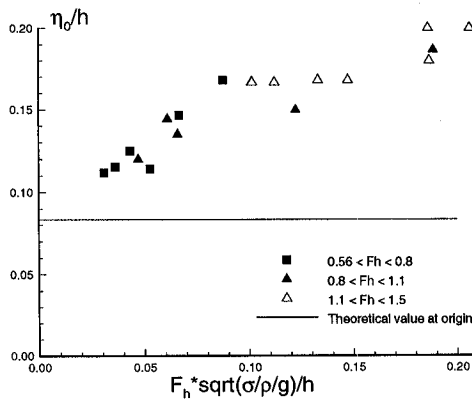


Figure 2: Initial elevation as a function of the surface tension parameter. $\alpha = 15^\circ$, $F_h = U/\sqrt{gh}$, $\sigma =$ surface tension.

For the wave elevation along the hull ($\hat{x} > 0$), the following three-dimensional correction should be added to the bow flow solution :

$$\Delta\eta = \frac{\alpha h}{\pi} \left[\hat{x} \ln \left(2\hat{x}(-\hat{x} + \sqrt{\hat{x}^2 + 1}) \right) - \hat{x} + \sqrt{\hat{x}^2 + 1} \right]$$

x/h	0 ⁻	0.05	0.1	0.15	0.2	0.3
$\pi\Delta\eta/(\alpha h)$	1.0	0.83	0.73	0.66	0.6	0.5

x/h	0.4	0.5	1.	2.	5.	∞
$\pi\Delta\eta/(\alpha h)$	0.43	0.38	0.22	0.12	0.05	0

Table 1: Numerical values of the wave profile correction.

However, this three-dimensional correction is not sufficient to completely explain the differences between experiments and the bow solution by Fontaine & Cointe (1997). One reason to this is surface tension effects like in fig. 2. There were not done measurements for the wave elevation along the hull for small surface tension parameter to see any trend for full scale situation. This need further investigations.

References

- [1] FALTINSEN, O.M. and ZHAO, R. (1991) : "Numerical prediction of ship motions at high forward speed", Phil. Trans. of the Royal Society, London (A), Vol. 334, pp. 241-252.
- [2] FONTAINE, E. and COINTE, R. (1997) : "A Slender Body Approach to Nonlinear Bow Waves", Phil. Trans. of the Royal Society, London (A).
- [3] FONTAINE, E. (1996) : "Simulation de l'écoulement potentiel engendré par un corps élané percant la surface libre à forts nombres de Froude", Thèse de Doctorat de l'Ecole Nationale des Ponts et Chaussées, Paris.
- [4] OGILVIE, T.F. (1972) : "The wave generated by a fine ship bow", Ninth Symp. Naval Hydrodynamics, Vol. 2, pp. 1483-1525.
- [5] SCLAVOUNOS, P. (1994) : "On the Intersection Near a Fine Ship Bow", Twentieth Symp. Naval Hydrodynamics, pp. 934-945.

DISCUSSION

Tuck E.O.: I applaud this study, which corrects a well-known deficiency in the 2.5 D theory, namely absence of a rise in FS at the bow. But I am not sure how it was achieved, since surely matching between the local bow flow and the 2.5 D expansion should have supplied a non-zero initial condition to the latter.

Fontaine E.: Thank you for your comments. The matchings have been performed using the classical technique of matched asymptotic expansions and the details of the procedure will be published soon. It appears that 3D effects arise in the composite solution which is the sum of the 2.5 D expansion and the local bow flow, subtracting the common part of the two expansions.